Anti-Cancer Drugs 1997, **8**, pp. 677–685

The loading rate determines tumor targeting properties of methotrexate–albumin conjugates in rats

Gerd Stehle,[1,2] Hannsjörg Sinn,[2] Andreas Wunder,[1,2] Hans Herrmann Schrenk,[2] Sandra Schütt,[1] Wolfgang Maier-Borst[2] and Dieter Ludwig Heene[1]

[1]First Department of Medicine, Faculty for Clinical Medicine Mannheim, University of Heidelberg, Germany.
[2]Department of Radiochemistry and Radiopharmacology, German Cancer Research Center Heidelberg, Germany.

Albumin dominates the plasma proteins in man. Following our observation that albumin turnover in rodent tumors is markedly increased, we will present evidence that albumin can be employed as an efficient carrier for targeting cytostatic agents like methotrexate (MTX) into tumors. The considerable discrepancy in the molecular weight of MTX (454 Da) and albumin (about 67 000 Da) tempted researchers to load multiple drug molecules on one carrier molecule. It was supposed that the optimal therapeutic efficacy of MTX protein conjugates could be achieved by increasing the number of the molecules of MTX attached to the carrier. In this paper we will show that only loading rates of close to 1 mol of the cytostatic drug MTX/mol of albumin offer optimal conditions for targeting MTX–albumin conjugates into rodent tumors. Conjugates bearing 5, 7, 10 and 20 molecules of MTX on average showed considerable alterations in the HPLC profiles of the conjugates compared to albumin. Conjugates carrying 5–20 mol MTX, tagged with a residualizing radiolabel, were efficiently trapped by the liver before reaching the tumor. The tumor uptake rates of these conjugates declined dramatically with an increasing molecular load of the cytotoxic drug linked to albumin. Competition experiments with maleylated bovine serum albumin and fucoidan revealed that scavenger receptors present on the cells of the liver monocyte macrophage system were involved in this process. For further preclinical and clinical studies, we chose MTX–albumin conjugates, derivatized at a molar ratio of 1:1. These conjugates enjoy the same favorable tumor targeting properties like albumin, e.g. high tumor uptake rates, low liver uptake rates and a very long biological half-life.

Key words: drug carriers, [^{111}In]DPTA, methotrexate, pharmacokinetics, pharmacology, residualizing labels, scavenger receptors, scintigraphy, Walker-256 carcinosarcoma.

Supported by research grants to GS from Forschungsfonds 1993-96 of the Faculty for Clinical Medicine Mannheim of Heidelberg University.

Correspondence to G Stehle Department of Radiochemistry and Radiopharmacology (FS 05), German Cancer Research Center, Im Neuenheimer Feld 280, 69120 Heidelberg, Germany. Tel: (+49) 6221-422485; Fax: (+49) 6221-422572

Introduction

Albumin dominates the plasma proteins of man. Following our recently published observation that albumin turnover in tumors is markedly increased, we will now present evidence that albumin can be employed as an efficient carrier for targeting cytostatic agents like methotrexate (MTX) into tumors.[1] The physiologic properties of albumin favors its use as a drug carrier. Albumin easily gains access to the interstitial space by leaving the vascular system via transcytosis.[2] The biological half-life of albumin in man amounts to 19 days and to 2.2 days in the rat.[3,4] During its life-time in man an average albumin molecule makes about 15 000 trips around the circulatory system, and about 15 trips through the extravascular space and back to the blood via the lymphatic system.[2] Thus, there will be multiple opportunities for the carrier to encounter proliferating tumor cells even in remote areas of the body. Proliferating tumor cells incorporate albumin by fluid-phase endocytosis. After lysosomal degradation low molecular weight amino acid nutrients are set free and, in the case of a drug–albumin conjugate, the conjugated cytotoxic drug as well. Further arguments favoring albumin are that albumin is not immunogenic or toxic. It is biodegradable and available in abundant amounts. More than other plasma protein, albumin resists denaturation by heat or by chemical reagents, allowing efficient virus inactivation and offering promising conditions for the conjugation of drugs.[2]

Although albumin has early been recognized as a drug carrier for MTX,[5,6] no albumin–drug conjugate has entered clinical use, so far. The discrepancy in the molecular weight of the chemotherapeutic drug and of albumin tempted researchers to load multiple drug molecules on one carrier molecule. It was supposed that the therapeutic efficacy of drug protein conju-

gates could be improved by increasing the number of drug molecules attached to the carrier. In this paper we will show that only a loading rate of about 1 mol of the cytostatic drug MTX/mol of albumin offers optimal conditions for targeting MTX–albumin conjugates into rodent tumors.

Materials and methods

Rat serum albumin (RSA; molecular weight 65 871 Da) and MTX (amethopterin; molecular weight 454.45 Da) were purchased from Sigma (Deisenhofen, Germany). All reagents like hydroxysuccinimide, diethylenetriaminepentaacetic acid, *N,N'*-Dicyclohexylcarbodiimide (DCC) and Trypan blue were purchased from Aldrich (Steinheim, Germany). Indium-111 was purchased from Du Pont de Nemours (Bad Homburg, Germany). Centricon ultrafiltration units from Amicon (Witten, Germany) were used for separation of the compounds. All products for tumor cell culture were purchased from Gibco/BRL (Eggenstein, Germany): standard RPMI 1640 medium, fetal calf serum, L-glutamine, penicillin–streptomycin solution (PenStrep), phosphate-buffered saline (Dulbecco's PBS) and Hanks balanced salt solution.

Preparation of the MTX–RSA conjugates

Conjugates from albumin and MTX were prepared by a slightly modified technique using carbodiimide as a linking agent, as published by Bures *et al.*[7] For the activation of MTX, DCC was used. A typical reagent mixture contained MTX at 20 mg/ml. To about 1 ml of this solution 14 mg DCC and 50 mg of *N*-hydroxysuccinimide were added. The formation of the activated methotrexate (MTX-SE) was completed after 12 h. Thin layer chromatography was performed as a control of activation efficiency. Silicagel 60 plates (5 × 20 cm) with a fluorescence indicator (Merck, Darmstadt, Germany) were used. The developing solvent was a mixture of ethyl acetate and methanol (75 : 25; v/v), running distance 10 cm. R_f values were 0.0 for MTX and 0.35–0.38 for MTX-SE. MTX-SE was slowly added to a solution of 20–50 mg RSA/ml (dissolved in 0.13 M sodium phosphate buffer, pH 7.4). The mixture was stirred for 30 min at room temperature and filtered with a Stericup® GV (0.22 μm low binding Duropore membrane; Millipore, Molsheim, France). The remaining low molecular weight reagents were separated by ultrafiltration using a membrane with an exclusion size of 30 000 Da. The addition of increasing amounts of activated MTX to RSA yielded conjugates with increasing loading rates. To achieve a loading rate of about 1 mol MTX/mol RSA, 15 mg of MTX was added to 1.5 g RSA. Average molar loading rates of 3, 5, 7, 10 and 20 mol MTX/mol RSA were achieved by adding 45, 75, 105, 150 and 300 mg of MTX to 1.5 g RSA. The respective binding rates of MTX to RSA were calculated after a photometric determination of the amount of unbound MTX in the filtrate. The concentration of MTX was determined by absorption at 370 nm in sodium bicarbonate buffer, 0.17 M, pH 8.5. The resulting conjugates were termed according to their average molar MTX loading rate MTX(1)–RSA, MTX(3)–RSA . . . MTX(20)–RSA. For the determination of the distribution patterns of MTX–RSA in tumor bearing rats, the RSA conjugates were tagged with a residualizing [^{111}In]DTPA label.

The coupling of DTPA to MTX–RSA was carried out after using DCC and hydroxysuccinimide (HSI) for DTPA activation. DTPA was dissolved in DMSO (20 mg/ml). Then a 1.5 M amount of DCC and a 5 M amount of HSI were added. After 12 h the formation of the succinimidylester of DTPA (DTPA-SE) was completed. The activated DTPA-SE was added to a commercially available albumin solution (20%). After 30 min of gentle stirring of the mixture, the remaining DCC and dicyclohexylurea were removed from DTPA–MTX–RSA by filtration (Stericup GV). The low molecular weight hydrophilic compounds were removed by an Amicon Ultrafiltration unit (30 kDa). For radiolabeling, 185 MBq $^{111}InCl_3$ (5 mCi) was mixed with 5 μl of a 0.2 M sodium citrate solution and then added to 10 mg DTPA–MTX(1–20)–RSA dissolved in 1 ml 0.17 M sodium bicarbonate. Unbound tracer was separated by a Centricon ultrafiltration C30 unit. The labeling yield was about 97%. An analytical HPLC control run of the purified [^{111}In]DTPA–RSA or [^{111}In]DTPA–MTX(1–20)–RSA tracers showed impurities of below 1%. The loading rate of the DTPA label was adjusted to a molar ratio of 1:1 with RSA. All conjugates were analyzed for protein and MTX content using a HPLC system equipped with two UV detectors adjusted to 280 nm for protein determination or to 370 nm for MTX. A LB506-C1 γ detector unit (Fa. Berthold, Wildbad, Germany) had been added for the detection of ^{111}In. Thus, it was possible to study the albumin, MTX and ^{111}In content of the conjugates simultaneously during one run. The HPLC system and the detailed procedures for analysis of protein conjugates have been published elsewhere.[8]

The conjugation technique did not lead to the formation of multimers of albumin. The HPLC profiles of the [^{111}In]DTPA–RSA and of [^{111}In]DTPA–MTX–RSA tracers derivatized with 1, 5 and 10 mol of MTX are shown in Figure 1(a–d). The same HPLC conditions

were used for all conjugates. The HPLC profile of radiolabeled RSA serving as a control is shown in Figure 1(a). Corresponding peaks were detected simultaneously at 280 nm (protein) and at a γ energy of 247 keV. The small peak at a retention time of 17 min was caused by a low amount of albumin dimers that was also present in the native RSA purchased from Sigma. The same protein peak was found for native RSA without a radiolabel, as well (data not shown). Figure 1(b) shows the pattern of [^{111}In]DTPA–MTX(1)–RSA, the conjugate with the lowest molar load of MTX analyzed at 280 nm (protein), 370 nm (MTX) and at a γ energy of 247 KeV. The shape of the protein curve of MTX(1)–RSA matched with native, unmodified RSA and with radiolabeled [^{111}In]DTPA–RSA. Substantial distortions in HPLC curves occurred after increasing the molar load of MTX to about 5–10 mol/mol of albumin and were documented simultaneously (Figure 1c–d).

Rat tumor model

Thirty-three female Sprague Dawley rats, weighing 200–250 g, were obtained from Zentrale Versuchstieranstalt, Hannover, Germany. The rats were kept under standard living conditions in the Central Animal Laboratory of the German Cancer Research Center, Heidelberg. The animal experiments had been approved by the German Federal Government (Regierungspräsidium Karlsruhe AZ 95/1991 and 100/1995 to G Stehle). As a tumor model we chose the Walker-256 carcinosarcoma. The Walker-256 cells had been obtained from the tumor cell bank of the German Cancer Research Center, Heidelberg. These cells had initially been passaged by ascites. In 1989 the tumor cells had been adapted to cell culture at the German Cancer Research Center and were stored at −196°C. The tumor cells were cultivated using a standard RPMI 1640 medium enriched with 10% (v/v) of heat-

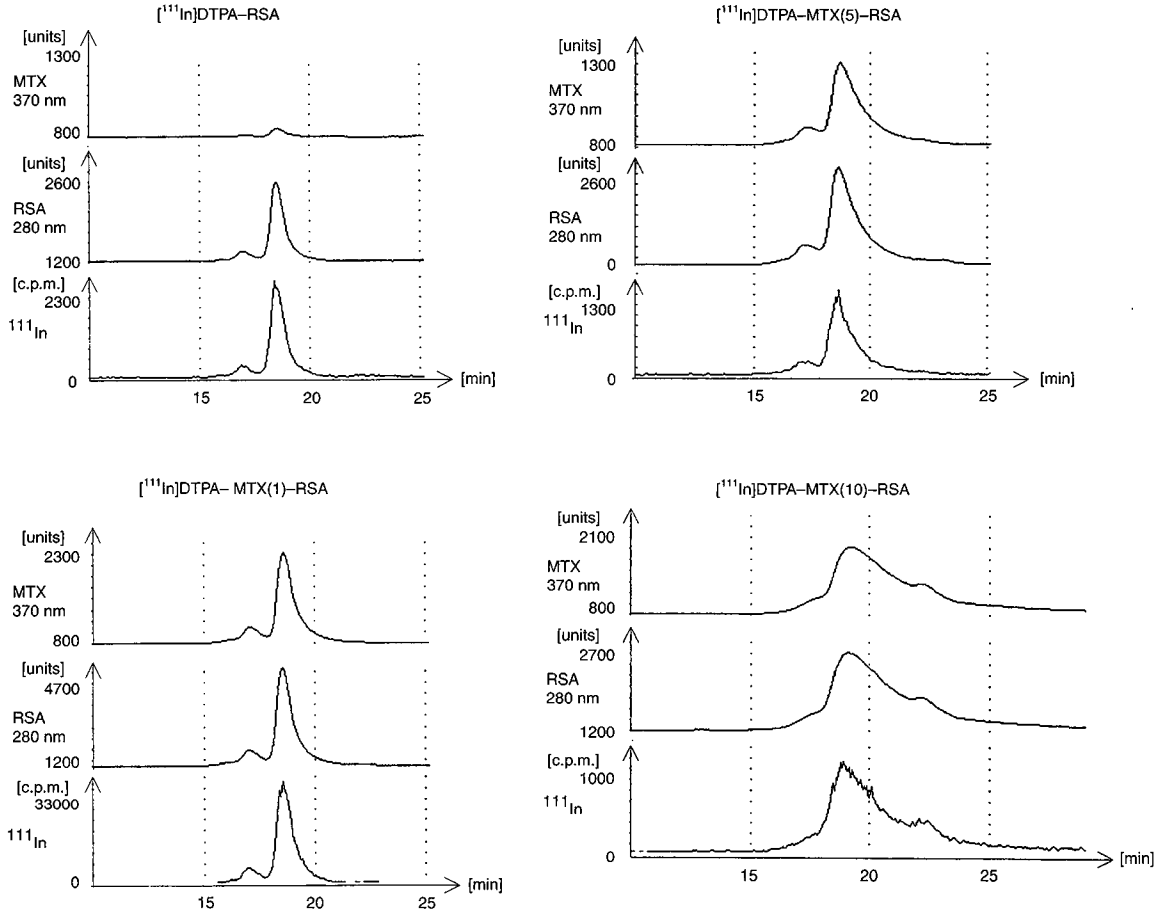

Figure 1. HPLC analysis of different RSA conjugates by simultaneous three-channel recording. The first channel detects MTX at 370 nm, the second channel RSA at 280 nm and the third channel the γ counts (c.p.m., at 247 keV) of the ^{111}In radiolabel. [^{111}In]DTPA–RSA served as a control. The HPLC curves for an increasing molar load (1, 5 and 10) of MTX per carrier molecule are shown.

inactivated fetal calf serum, L-glutamine and PenStrep. The culture medium was changed every 48 h and a final concentration of about 1×10^6 cells/ml was attained. At least five cell passages were carried out before transferring the tumor to the rats. Viable cells were counted after Trypan blue uptake. Female SD rats received an intramuscular injection of 3×10^6 viable Walker-256 cells at their left hind leg, diluted in Hanks balanced salt solution to a volume of 200 μl. The experiments were started when the tumors had reached an estimated weight of about 8 g or about 3% of the respective body weight of the rats.

Throughout the experiments the tumor-bearing rats were anaesthetized by a mixture of halothane, N_2O and O_2 (1.5%/60%/38%). The rats were placed in a prone position on a high energy multihole collimator (420 keV) of a 10 inch γ camera (Pho-Gamma IV; Searle-Siemens, Erlangen, Germany). For the on-line evaluation of the data, a computer system specially adapted to the γ camera was used (Gaede Medworker, Gaede, Freiburg, Germany). To study the distribution of the tracer substance in the animals static images (5 min) were registered 5, 10 and 20 min and 4 and 24 h after tracer injection. The regions of interest (ROI) were marked, and the content of radioactivity in heart, liver, kidneys, urinary bladder, the tumor and the carcass was evaluated. The percentage of activity present in each region of interest was calculated from the counts of that area in relation to the whole body count rate. All substances were administered by an i.v. injection into a lateral tail vein. Eighteen tumor-bearing rats were randomly divided into six groups. The rats of each group received an i.v. injection of 100 μg of [^{111}In]DTPA–MTX–RSA (3.7 MBq; 100 μCi) with an increasing molar load of MTX [MTX(1)–RSA, MTX(3)–RSA, MTX(5)–RSA, MTX(7)–RSA, MTX(10)–RSA and MTX(20)–RSA]. At 5, 10 and 20 min and 4 and 24 h after tracer administration triplicate blood samples (20 μl per sample) were drawn after incising the tail tip. A reference curve was prepared using triplicate serial dilutions of the tracer substance. After each blood sampling procedure the initial standard tracer dilution was recounted to adjust for the radioactive decay of ^{111}In. The equation 'blood volume=0.06 × body weight+0.77' was used to estimate the blood volume of the rats.[9] From these data the percentage of the injected radioactivity present in the blood at different times was calculated. The blood loss of the animals was less than 1 ml or below 4% of the respective total blood volume. After the final scintigraphy and blood sampling the animals were sacrificed after CO_2 narcosis and the organs removed. After determination of the weight, the radioactivity of the samples was measured in a γ counter. At the same time the respective standard dilutions of the tracer were counted to adjust for the radioactive decay of ^{111}In. The results were expressed as percent of radioactivity uptake per organ based on the initially injected dose. The following organs were examined: heart, liver, kidneys, spleen, lungs, stomach, intestines, colon, tumor and carcass (muscles, bone, skin).

Fifteen tumor-bearing rats were chosen for studying the receptor-mediated liver monocyte macrophage system (MMS) uptake of highly loaded albumin conjugates [MTX(10)–RSA]. These rats were randomly allocated to three groups. Five rats of the control group received an i.v. injection of 100 μg of [^{111}In]DTPA–MTX(10)–RSA (3.7 MBq, 100 μCi). Fucoidan (purchased from Sigma) and mal-BSA were chosen for receptor blocking. Mal-BSA had been prepared by maleylating BSA with maleic acid anhydride.[10–12] The five rats of the fucoidan group received 5 mg fucoidan i.v. 5 min prior to the injection of the [^{111}In]DTPA–MTX(10)–RSA tracer. Another five rats of the mal-BSA group received 5 mg maleylated bovine serum albumin 5 min prior to tracer administration. Scintiscans were performed over 1 h and then all animals were sacrificed. The uptake rates of radioactivity were evaluated for blood, tumor and liver.

Statistics

For the descriptive analysis of the data mean values and standard deviation were calculated. The area under curve (AUC) was determined using the computer program TOPFIT 2.0 (Thomae Optimized Pharmacokinetic Fitting Program for the PC[13]). The AUC was calculated employing the logarithmic trapezoidal rule and the exponential extrapolation of the first two data points to the time of administration was calculated. For determination of the total AUC (0 h to ∞) the terminal elimination constant λ_z was used from the last point of the curve.

Results

Kinetics of MTX–RSA conjugates derivatized with MTX in molar ratios from 1 to 20

To study the impact of the loading rate on the *in vivo* pharmacokinetics of MTX–RSA conjugates, 18 tumor-bearing rats were divided into six groups. Three rats of each group received i.v. injections of radiolabeled MTX–RSA conjugates. The MTX–RSA conjugates had

been derivatized with increasing molar ratios of about 1:1, 1:3, 1:5, 1:7, 1:10 up to 1:20. Sequential scintigraphy was performed and blood samples were collected. After 24 h organs and tumors were removed for γ counting.

Figure 2 shows the radiokinetics in blood for the different MTX–RSA conjugates. A circulation time equal to the native RSA tracer was found for MTX(1)–RSA. MTX(5)–RSA showed a slightly reduced circulation time. Conjugates derivatized with 7, 10 or 20 molecules of MTX were rapidly removed from circulation. AUC calculations revealed a relative plasma presence of 0.97 for MTX(3)–RSA, 0.86 for MTX(5)–RSA, 0.62 for MTX(7)–RSA, 0.33 for MTX(10)–RSA and 0.09 for MTX(20)–RSA, compared to 1.0 for MTX(1)–RSA (Table 1).

Scintigraphy was used to detect the uptake sites of radiolabeled MTX–RSA conjugates with an increasing molar load of MTX (Figure 3). Four rats bearing tumors of the same size received injections either with radiolabeled MTX(1)–RSA, MTX(5)–RSA, MTX(7)–RSA or MTX(10)–RSA. The scintigraphic distribution pattern of MTX(1)–RSA was like that of radiolabeled RSA. After 24 h considerable amounts of the MTX(1)–RSA conjugate were still present in circulation as shown by the delineation of the heart region in the first scintigram in Figure 3. Some activity was also found in the liver and kidney regions. The major site of MTX(1)–RSA tracer accumulation was the tumor. The distribution pattern of conjugates derivatized with 5 mol MTX/mol RSA already changed and the liver

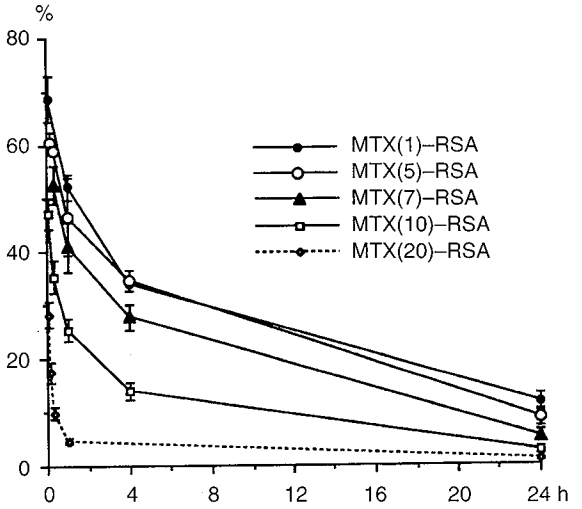

Figure 2. Radiokinetics measured in blood after i.v. administration of [^{111}In]DTPA–MTX–RSA conjugates derivatized with 1, 5, 7, 10 and 20 mol MTX/mol RSA. The percentage of radioactivity was calculated based on the initially administered dose (all rats bearing a Walker-256 carcinosarcoma with approximately the same tumor size, n=3, mean, SD).

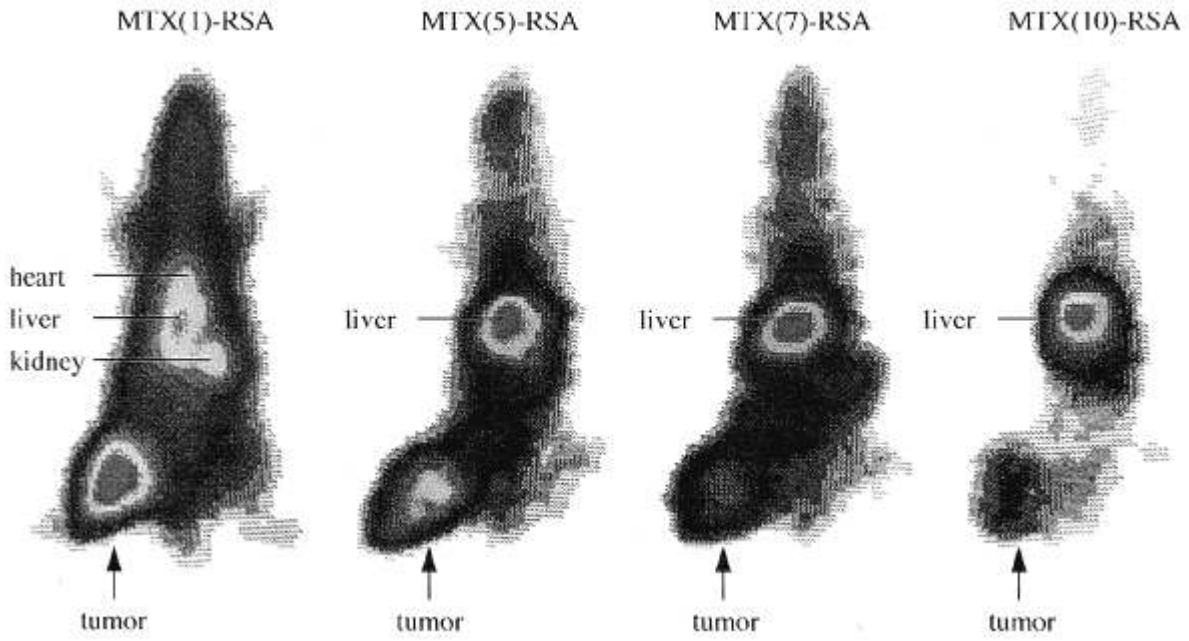

Figure 3. Scintigrams of four rats bearing a Walker-256 carcinosarcoma of the same size 24 h after the injection of MTX–RSA conjugates derivatized with an increasing molar load of MTX (1, 5, 7 and 10 mol MTX/mol RSA). With increasing molar load the conjugates are predominately trapped in the liver and no longer by the tumor (the color code for high amounts of radioactivity is red, with gradings from yellow, green to blue for the lowest amounts).

became the major uptake site *in vivo*. The tumor uptake for MTX(5)–RSA conjugates declined. Further significant losses in tumor uptake were observed for MTX(7)–RSA and MTX(10)–RSA. The liver was the dominating trapping site for MTX(10)–RSA conjugates and tumor uptake became negligible.

With an increasing molar load of MTX linked to the carrier protein, scintigraphy had revealed a distribution of the conjugates from tumor to liver—an observation that was confirmed by quantifying the tracer uptake rates after organ and tumor removal. The liver uptake already doubled from 6 to 12% of the injected dose after 24 h, if MTX(1)–RSA and MTX(3)–RSA were compared (Figure 4). The addition of another few more molecules of MTX to RSA caused steep increases in liver uptake (MTX(5)–RSA 18%, MTX(7)–RSA 20%, MTX(10)–RSA 43%, and MTX(20)–RSA 60%). At the same time the tumor uptake rates dropped from about 25% of the initially injected dose of MTX(1)–RSA to about 2% of the injected dose for MTX(20)–RSA.

Competition experiments to study the liver uptake of MTX(10)–RSA

The alteration of the HPLC profiles and the typical change in organ and tumor distribution lead to the conclusion that the monocyte macrophage system (MMS) of the rat liver might have been involved in removing highly loaded MTX-RSA conjugates from circulation. Prime suspects responsible for removal of denatured polyanionic material are macrophage scavenger receptors. The injection of the blocking agents fucoidan or mal-BSA took place 5 min before MTX(10)–RSA tracer administration, thus competing with the conjugates for scavenger receptor-mediated liver uptake. In a control experiment radiolabeled MTX(10)–RSA material was injected alone. About 47% of this material was trapped by the liver (Figure 5). Preinjection of fucoidan reduced the liver uptake rate by 22%. The administration of mal-BSA blocked MTX(10)–RSA most efficiently out of the liver diminishing the uptake rate to about 10% compared to 47% in the control group. Receptor-mediated endocytosis by cells of the liver MMS, involving the group of

Table 1. AUC calculations and relative amounts of circulating MTX–RSA conjugates with substitution degrees from 1 to 20 mol MTX

	AUC (%*h)		AUC (relative)	
	0 to 24 h	0 to ∞	0 to 24 h	0 to ∞
MTX(1)–RSA	602.6	774.8	1.00	1.00
MTX(3)–RSA	591.4	752.9	0.98	0.97
MTX(5)–RSA	551.5	663.4	0.92	0.86
MTX(7)–RSA	421.7	478.1	0.70	0.62
MTX(10)–RSA	229.9	255.6	0.38	0.33
MTX(20)–RSA	64.4	72.8	0.11	0.09

The amount (%) of the tracers present in blood was used for the calculations. The AUC was estimated employing the logarithmic trapezoidal rule. For determination of the total AUC (0 h to ∞) the terminal elimination constant λ_Z was used.

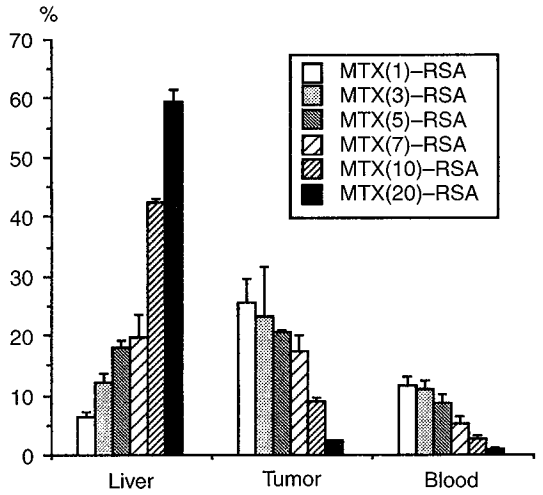

Figure 4. Liver tumor uptake rates and presence in circulation of [^{111}In]DTPA–MTX–RSA conjugates derivatized with 1, 3, 5, 7, 10 and 20 mol MTX/mol RSA 24 h after i.v. injection. The amount of radioactivity is shown as percent of the initially injected tracer amount (all rats bearing a Walker-256 carcinosarcoma, n=3, mean, SD).

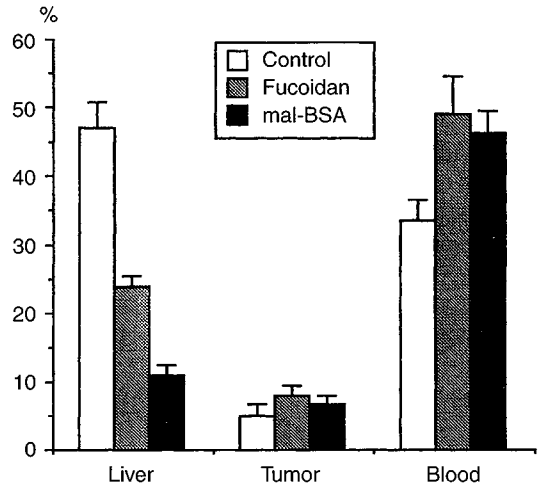

Figure 5. Uptake and circulation rates of an [^{111}In]MTX(10)–RSA conjugate measured in the liver, in the tumor and in blood without and after blocking the scavenger receptors of the liver MMS with fucoidan or mal-BSA. Liver, tumor and blood had been removed 1 h after tracer injection (all rats bearing Walker 256-carcinosarcomas, n=5, mean, SD).

scavenger receptors, seemed to be responsible for the efficient hepatic removal of highly loaded denatured MTX–RSA conjugates.

Discussion

Throughout the last three decades it was attempted to exploit albumin as a carrier system for cytostatic drugs like MTX. To our knowledge the experiments with MTX–albumin conjugates remained in the preclinical state, although cell culture experiments had shown promising results. Drug resistance due to transport deficiencies for native MTX was overcome by MTX–albumin conjugates in tumor cell culture.[14–16] From the beginning the discrepant molecular weights of MTX and of albumin directed all efforts to improve the therapeutic efficacy of these conjugates on raising the molecular load from initially about 10 mol MTX conjugated per albumin molecule to MTX–albumin conjugates carrying 56 mol MTX/mol albumin. MTX–albumin conjugates with loading rates close to a molar ratio of 1:1 have not been studied, so far.[5,17–22]

For our experiments on albumin and its MTX conjugates we chose a residualizing [^{111}In]DTPA radiolabel. Initially proposed by S Thorpe and RC Pittman in the 1980s, residualizing or cumulative radiolabels have been increasingly used to locate catabolic sites of proteins *in vivo*.[23] A common feature of residualizing protein labels is that they remain trapped at the cellular site of degradation with intracellular half-lives up to 5 days helping to localize the degradation sites of proteins.[23–25] Recent studies had identified the intracellularly trapped metabolites of [^{111}In]DTPA–labeled proteins. [^{111}In]DTPA–lysine was found responsible for the intralysosomal accumulation of tracer radioactivity after protein degradation.[26,27]

A large spectrum of [^{111}In]DTPA–MTX–RSA conjugates derivatized with 1, 3, 5, 7, 10 and 20 mol MTX was prepared to study *in vivo* tumor targeting. HPLC analysis revealed that conjugates bearing five MTX residues or more showed profiles decisively different from those obtained for native RSA. With increasing derivatization degree a distortion of the HPLC curves occurred, indicating the progressive alterations of the carrier molecule. These findings are consistent with data published by Halbert *et al.*[19] on the physicochemical characterization of highly derivatized MTX(5–15)–BSA conjugates, showing that the shape and hydration properties had suffered considerably during conjugation procedures. With an increase in MTX loading of the conjugates the frictional ratio of the conjugates deteriorated compared to native BSA, indicating the presence of intramolecular cross-linking of the carrier molecule, as well. In addition, albumin polymers resulting from intermolecular cross-linking were detected by SDS–PAGE analysis of MTX(5–15)–BSA conjugates and attributed to known chemical properties of reagents like carbodiimide, used for the coupling of MTX to proteins.[28,29] We did not observe polymer formation during our conjugation procedure. The small amount of albumin dimers detected by HPLC was already present in native RSA. Dimer formation is attributed to the pasteurization of albumin and can be found in all albumin preparations. Negative effects caused by albumin dimers are not known.[2]

In this study we have shown that the i.v. administration of highly loaded denatured MTX–RSA conjugates resulted in a rapid removal from the circulation. The liver was identified as the dominant trapping site for all conjugates with loading ratios exceeding 1 molecule of MTX per carrier molecule. About 6% of the injected dose of radiolabeled MTX(1)–HSA was found in the liver after 24 h. The loading of the albumin carrier with 3 mol MTX already doubled the hepatic uptake. More than 60% of the initially injected amount of MTX(20)–RSA was trapped by the liver. Consequently, the tumor uptake rates declined from 25% of the initially injected dose of MTX(1)–RSA to less than 2% of MTX(20)–RSA. The efficient hepatic uptake of MTX(5–20)–RSA conjugates raised the possibility that receptor-mediated uptake mechanisms in the liver MMS might be involved.

With an increasing molar load of MTX the albumin conjugates will become more and more polyanionic. The charge will be altered by conversion of an amine to an amide function and by addition of a negative charge due to the second carboxyl group of the glutamate moiety of MTX. Therefore our search focused on the heterogeneous group of scavenger receptors, mainly present on Kupffer cells of the liver MMS. Scavenger receptors are known to be involved in the removal of a variety of polyanionic compounds from circulation such as extracellular debris including pathogenic material like lipopolysaccharides or oxidized low density lipoprotein.[30–32] These receptors also exhibit a broad ligand specificity for a variety of other polyanionic ligands, such as fucoidan, dextran sulfate, maleylated bovine serum albumin, polyvinyl sulfate, heparins or heparin protamine aggregates.[33–38]

In a competition experiment to identify the mechanism underlying the high hepatic uptake rates of MTX(10)–RSA, we used two known scavenger receptor ligands, fucoidan and mal-BSA. Preinjection of fucoidan decreased the hepatic uptake rates for MTX(10)–RSA from about 50% of the injected dose to about 25%. Mal-BSA was even more efficient, reducing the hepatic uptake to only 10%. These data

clearly indicate that liver macrophages bearing scavenger receptors are involved in the premature disappearance of highly loaded MTX–RSA conjugates from blood. The phenomenon of a scavenger receptor-mediated liver uptake has also been described for conjugates of the anti-inflammatory drug naproxen and human serum albumin after derivatization with a 20 M excess of negatively charged naproxen.[39] Recent data on the function of macrophage scavenger receptors suggest that these receptors participate in host defense mechanisms.[32] Scavenger receptor-mediated targeting of maleylated polyanionic diphtheria toxoid into cells of the liver MMS lead to an enhanced immunogenicity of the toxoid and to the formation of toxoid antibodies without using additional adjuvants.[40] MMS entrapment of massive amounts of denatured cytotoxic MTX–protein conjugates might exert deleterious effects on macrophage function, as well.

Overloaded MTX–albumin conjugates exhibit decisive shortcomings, that might have been responsible for their preclinical failure. MTX(1)–albumin conjugates offered the best tumor targeting properties and the lowest liver uptake rates of all conjugates tested in our study. For further preclinical and clinical studies we chose the MTX–albumin conjugate, derivatized at a molar ratio of about 1:1.[41–45]

Acknowledgments

The authors thank H Löhrke from the tumor cell bank of the German Cancer Research Center Heidelberg for providing Walker-256 carcinosarcoma cells. We gratefully acknowledge the assistance of D Hoff-Biederbeck and C Blum cultivating the tumor cells.

References

1. Stehle G, Sinn H, Wunder A, *et al.* Plasma protein (albumin) catabolism by the tumor itself—implications for tumor metabolism and the genesis of cachexia. *Crit Rev Oncol Hematol* 1997; in press.
2. Peters T. *All about albumin: biochemistry, genetics and medical applications.* San Diego, CA: Academic Press 1996.
3. Peters T. Serum albumin. *Adv Protein Chem* 1985; **37:** 161–245.
4. Katz G, Bonorris G, Golden S, Sellers AL. Extravascular albumin mass and exchange in rat tissues. *Clin Sci* 1970; **39:** 705–24.
5. Magnenat G, Schindler R, Isliker H. Transport d'agents cytostatiques par les protéines plasmatiques: III. Activité antitumorale *in vitro* de conjugués cytostatique-azoprotéines. *Eur J Cancer* 1969; **5:** 33–40.
6. Jacobs SA, d'Urso-Scott M, Bertino JR. Some biochemical and pharmacologic properties of amethopterin-albumin. *Ann NY Acad Sci* 1971; **186:** 284–6.
7. Bostik J, Bures L, Spundova M. The use of protein as a carrier of methotrexate for experimental cancer chemotherapy. IV. Therapy of murine melanoma B16 by human serum albumin–methotrexate derivative. *Neoplasma* 1988; **35:** 343–9.
8. Sinn H, Schrenk HH, Friedrich EA, Schilling U, Maier Borst W. Design of compounds having an enhanced tumour uptake, using serum albumin as a carrier. Part I. *Int J Radiat Appl Instrum B* 1990; **17:** 819–27.
9. Lee HB, Blaufox MD. Blood volume in the rat. *J Nucl Med* 1985; **26:** 72–6.
10. Butler PJG, Hartley BS. Maleylation of amino groups. *Methods Enzymol* 1972; **25:** 191–9.
11. Imber MJ, Pizzo SV, Johnson WJ, Adams DO. Selective diminution of the binding of mannose by murine macrophages in late stages of activation. *J Biol Chem* 1982; **257:** 5129–35.
12. Ottnad E, Via DP, Frübis J, *et al.* Differentiation of binding sites on reconstituted hepatic scavenger receptors using oxidized low-density lipoprotein. *Biochem J* 1992; **281:** 745–51.
13. Heinzel G, Woloszczack R, Thomann P. *TOPFIT 2.0: Pharmacokinetic and pharmacodynamic data analysis system for the PC.* Stuttgart: Gustav Fischer: 1993.
14. Chu BC, Fan CC, Howell SB. Activity of free and carrier-bound methotrexate against transport-deficient and high dihydrofolate dehydrogenase-containing methotrexate-resistant L1210 cells. *J Natl Cancer Inst* 1981; **66:** 121–4.
15. Chu BC, Howell SB. Differential toxicity of carrier-bound methotrexate toward human lymphocytes, marrow and tumor cells. *Biochem Pharmacol* 1981; **30:** 2545–52.
16. Smyth MJ, Pietersz GA, McKenzie IF. The mode of action of methotrexate-monoclonal antibody conjugates. *Immunol Cell Biol* 1987; **65:** 189–200.
17. Chu BCF, Whiteley JM. High molecular weight derivatives of methotrexate as chemotherapeutic agents. *Mol Pharmacol* 1976; **13:** 80–8.
18. Shen WC, Ryser HJ. Selective killing of Fc-receptor-bearing tumor cells through endocytosis of a drug-carrying immune complex. *Proc Natl Acad Sci USA* 1984; **81:** 1445–7.
19. Halbert GW, Florence AT, Stuart JF. Characterization of *in-vitro* drug release and biological activity of methotrexate–bovine serum albumin conjugates. *J Pharm Pharmacol* 1987; **39:** 871–6.
20. Bures L, Bostik J, Motycka K, Spundova M, Rehak L. The use of protein as a carrier of methotrexate for experimental cancer chemotherapy. III. Human serum albumin–methotrexate derivative, its preparation and basic testing. *Neoplasma* 1988; **35:** 329–42.
21. Bures L, Lichy A, Bostik J, Spundova M. The use of protein as a carrier of methotrexate for experimental cancer chemotherapy. V. Alternative method for preparation of serum albumin–methotrexate derivative. *Neoplasma* 1990; **37:** 225–31.
22. Kim CK, Hwang SJ, Lee MG. The organ targetability of small and large albumin microspheres containing free and HSA conjugated methotrexate. *Int J Pharm* 1993; **89:** 91–102.
23. Thorpe SR, Baynes JW, Chroneos ZC. The design and application of residualizing labels for the studies of protein catabolism. *FASEB J* 1993; **7:** 399–405.

24. Lucas KL, Baynes JW, Thorpe SR. Intracellular processing of residualizing labels in different cell types *in vitro*. *J Cell Physiol* 1990; **142:** 581–5.
25. Tassin MT, Lang T, Antoine JC, Hellio R, Ryter A. Modified lysosomal compartment as carrier of slowly and non-degradable tracers in macrophages. *Eur J Cell Biol* 1990; **52:** 219–28.
26. Rogers BE, Franano FN, Duncan JR, *et al.* Identification of metabolites of ^{111}In-diethylenetriaminepentaacetic acid-monoclonal antibodies and antibody fragments *in vivo*. *Cancer Res* 1995; **55:** 5714s–20s.
27. Arano Y, Mukai T, Akizawa H, *et al.* Radiolabeled metabolites of proteins play a critical role in radioactivity elimination from the liver. *Nucl Med Biol* 1995; **22:** 555–64.
28. Halbert GW, Florence AT. Physiochemical characterization of methotrexate–bovine serum albumin conjugates. *J Pharm Pharmacol* 1989; **41:** 222–6.
29. Timkovich R. Polymerisation side reactions during protein modifications with carbodiimide. *Biochim Biophys Acta* 1977; **74:** 1463–8.
30. Hampton RY, Golenbock DT, Penman M, Krieger M, Raetz CR. Recognition and plasma clearance of endotoxin by scavenger receptors. *Nature* 1991; **352:** 342–4.
31. Acton S, Resnick D, Freeman M, Ekkel Y, Ashkenas J, Krieger M. The collagenous domains of macrophage scavenger receptors and complement component C1q mediate their similar, but not identical, binding specificities for polyanionic ligands. *J Biol Chem* 1993; **268:** 3530–7.
32. Krieger M, Acton S, Ashkenas J, Pearson A, Penman M, Resnick D. Molecular flypaper, host defense, and atherosclerosis. Structure, binding properties, and functions of macrophage scavenger receptors. *J Biol Chem* 1993; **268:** 4569–72.
33. Takata K, Horiuchi S, Morino Y. Scavenger receptor-mediated recognition of maleylated albumin and its relation to subsequent endocytic degradation. *Biochim Biophys Acta* 1989; **984:** 273–80.
34. Haberland ME, Tannenbaum CS, Williams RE, Adams DO, Hamilton TA. Role of the maleyl-albumin receptor in activation of murine peritoneal macrophages *in vitro*. *J Immunol* 1989; **142:** 855–62.
35. Zhang H, Yang Y, Steinbrecher UP. Structural requirements for the binding of modified proteins to the scavenger receptor of macrophages. *J Biol Chem* 1993; **268:** 5535–42.
36. Stehle G, Friedrich EA, Sinn H, *et al.* Hepatic uptake of a modified low molecular weight heparin in the rat. *J Clin Invest* 1992; **90:** 2110–6.
37. Stehle G, Wunder A, Sinn H, *et al.* Complexes of a modified low molecular weight heparin with protamine are predominantly cleared by a macrophage scavenger receptor mediated process in rats. *J Surg Res* 1995; **58:** 197–204.
38. Wunder A, Stehle G, Sinn H, *et al.* The injection of heparin prolongs plasma clearance of oxidized low density lipoprotein in the rat. *Thromb Res* 1995; **78:** 139–49.
39. Franssen EJ, Jansen RW, Vaalburg M, Meijer DK. Hepatic and intrahepatic targeting of an anti-inflammatory agent with human serum albumin and neoglycoproteins as carrier molecules. *Biochem Pharmacol* 1993; **45:** 1215–26.
40. Abraham R, Singh N, Mukhopadhyay A, Basu SK, Bal V, Rath S. Modulation of immunogenicity and antigenicity of proteins by maleylation to target scavenger receptors on macrophages. *J Immunol* 1995; **154:** 1–8.
41. Stehle G, Sinn H, Wunder A, *et al.* Albumin catabolism by tumors. *ECCO 9* 1997; A 795 (abstr).
42. Stehle G, Sinn H, Wunder A, *et al.* Tumor uptake of MTX–albumin conjugates in rats. *ECCO 9* 1997; A 808 (abstr).
43. Wunder A, Stehle G, Sinn H, *et al.* Radiokinetics of MTX–albumin conjugates in rats. *ECCO 9* 1997; A 794 (abstr).
44. Wunder A, Stehle G, Sinn H, *et al.* Antitumor activity of MTX–HSA conjugates in rats. *ECCO 9* 1997; A 800 (abstr).
45. Hartung G, Stehle G, Sinn H, *et al.* Phase-1 trial of a methotrexate–albumin conjugate (MTX–HSA) in cancer patients. *ECCO 9* 1997; 1129 (abstr).

(Received 13 June 1997; accepted 26 June 1997)